FIRST TEST RESULTS OF HALF-REENTRANT SINGLE-CELL SUPERCONDUCTING CAVITIES*

M. Meidlinger†, J. Bierwagen, S. Bricker, C. Compton, T. Grimm
W. Hartung, M. Johnson, J. Popielarski, L. Saxton, R. York
National Superconducting Cyclotron Laboratory, East Lansing, Michigan, USA
P. Kneisel, Thomas Jefferson National Accelerator Facility, USA
E. Zaplatin, Forschungszentrum Jülich, Germany

Abstract

Particle physicists are on the verge of reaching a new frontier of physics, the Terascale, named for the teravolts of kinetic energy per particle required to explore this region. To meet the demand for more beam energy, superconducting cavities need to achieve higher accelerating gradients. It is anticipated that niobium cavities will reach a performance limit as the peak surface magnetic field approaches the critical magnetic field. "Low-loss" [1] and "reentrant" [2] cavity designs are being studied at CEBAF, Cornell, DESY, and KEK, with the goal of reaching higher gradients via lower surface magnetic field, at the expense of higher surface electric field. At present, cavities must undergo chemical etching and high-pressure water rinsing to achieve good performance. While these surface treatment methods have been effective for low-loss and reentrant single-cell cavity designs, it is not clear whether the same methods will be adequate for multi-cell versions.

A "half-reentrant" cavity shape has been designed with RF parameters similar to the low-loss and reentrant cavities, but with the advantage that the same surface preparation should be reliable for multi-cell half-reentrant cavities. Two 1.3 GHz prototype single-cell half-reentrant cavities have been fabricated and tested at Michigan State University (MSU). One of the cavities was post-purified, etched via buffered chemical polishing, and tested at Thomas Jefferson National Accelerator Facility (TJNAF), reaching a maximum accelerating gradient of 35 MV/m. The half-reentrant cavity concept, design, fabrication, and first test results are presented.

INTRODUCTION

The concept and RF optimization of the half-reentrant cavity has been previously published [3]. The goal of the half-reentrant cavity is to provide similar electromagnetic performance as both low-loss and reentrant cavity designs (Table 1), but be able to be adequately cleaned with current technology, and therefore reliably reach high accelerating gradients.

* Work supported by the National Science Foundation.
† meidlinm@nscl.msu.edu

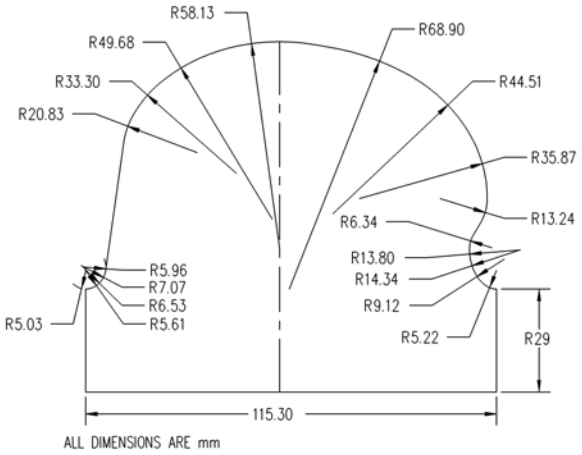

Figure 1: Mid-cell shape of fabricated half-reentrant cavity.

Design Shape

The previously published half-reentrant shape was made more complex at the end of 2005. In the original design shape [3], the non-reentrant half of the cavity was comprised of two ellipses connected by a straight section, which is typical of elliptical cavity shapes. The reentrant half of the cavity consisted of two ellipses in the iris region which were connected via a straight segment to one ellipse in the equatorial region. In the final design, every ellipse was replaced by a series of circular arcs as seen in Figure 1. This gives both the ability to adjust the surface electric and magnetic fields on a finer scale than previously

Table 2: Parameters of the fabricated single-cell half-reentrant cavity.

Parameter	Value
frequency	1288.6 MHz
wall angle	8°
E_{peak}/E_{acc}	2.27
B_{peak}/E_{acc}	3.52 $\frac{mT}{MV/m}$
R/Q	141 Ω
G	283 Ω
$(R/Q) \cdot G$	40102 Ω^2
r_i	2.9 cm

Table 1: Parameters of the previously proposed half-reentrant inner cell, designed with ellipses, compared to the fabricated cell, designed with circular arcs as shown in Figure 1. Two other designs proposed for the ILC are shown as a comparison.

		Half-Reentrant Ellipses [3]	Half-Reentrant Arcs (Fabricated)	Cornell Reentrant [4]	DESY/KEK Low-Loss [1]
frequency	[MHz]	1300	1299	1300	1300
wall angle	[°]	6	8	-	0.165
E_{peak}/E_{acc}	[-]	2.38	2.41	2.28	2.36
B_{peak}/E_{acc}	$[\frac{mT}{MV/m}]$	3.60	3.55	3.54	3.61
R/Q	[Ω]	135	136	121	134
G	[Ω]	283	285	280	284
$(R/Q) \cdot G$	[Ω^2]	38021	38796	41208	37970
k_{cc}	[%]	1.51	1.47	1.57	1.52
r_i	[cm]	2.97	2.90	3.00	3.00

possible in addition to adjusting the surface electric field independently from the surface magnetic. The iris radius was decreased from 29.7 mm to 29 mm to improve the electromagnetic performance and the non-reentrant wall angle was increased from 6° to 8° to allow for better fluid drainage. With a maximum surface magnetic field of 180 mT, the maximum theoretical accelerating gradient for a mid-cell is 50.7 MV/m.

MULTIPACTING SIMULATIONS

Multipacting simulations were completed using SUPERLANS [5, 6] and Multip [7]. SUPERLANS is first used to calculate the electromagnetic field distribution for the mode of interest throughout the cavity. Multip then uses this field table to calculate the Lorentz force and subsequent trajectory of an electron emitted from a point with a given velocity and emission angle, taking into account relativistic effects.

For multipacting simulations, primary electrons were emitted in 0.1 cm increments throughout the cavity surface, excluding the beam pipes. The peak surface electric field was varied from 0.05 MV/m to 150 MV/m in 0.05 MV/m steps. If an electron impacted the cavity wall with a kinetic energy between 20 eV and 3000 eV, it created a secondary electron, and the simulation continued. For each combination of field level and initial location, primary electrons were released at 100 different phases.

The initial electron kinetic energy values used were 0, 1, 2, and 3 eV. For initial electron kinetic energies of 0, 1, and 3 eV, an emission angle of 0° was used. The emission angle is measured from the normal of the cavity surface. For an initial electron kinetic energy of 2 eV, which corresponds to the most likely energy of an emitted electron, the emission angle was varied from $-30°$ to $+30°$ in 15° increments. In total, there were eight combinations of initial electron kinetic energy and initial emission angle. In reality, secondary electrons are emitted with a probabilistic distribution of initial kinetic energies and emission angles. However, the initial energy and emission angle are not chosen through any statistical model in the simulation, but are set by the user. The most likely initial kinetic energy is 2 eV, and the most probable emission angle is 0°. Therefore, after the simulations are completed, the computed results must be sifted through. Multipacting due to an initial kinetic energy of 2 eV and emission angle of 0° will be more likely to occur in reality than other initial conditions.

Multipacting simulations were completed for the single-cell half-reentrant cavity prototype and the mid-cell geometry. For the eight initial conditions used for the primary electron, only one case led to a potential multipacting barrier for a cavity that is moderately clean. We define a moderately clean cavity surface as one where the secondary emission coefficient is greater than 1 for an impacting electron energy between 40 eV and 1000 eV as explained in [8]. The multipacting was found to be a two-point multipacting barrier in the region of 45 MV/m $< E_{peak} <$ 70 MV/m, with the final impacting electron kinetic energy reaching 47 eV for an initial electron energy of 3 eV and emission angle of 0°. Since the maximum final impacting electron kinetic energy is relatively low, a possible soft multipacting barrier was predicted.

Testing of the cavities did not show any indications of multipacting, which is in good agreement with the cavity surface being adequately cleaned. Since the mid-cell multipacting simulations are not significantly different from the single-cell simulations, we do not anticipate a hard multipacting barrier for a multi-cell half-reentrant cavity.

FABRICATION

Parts for three single-cell half-reentrant cavities were fabricated, and two single-cell cavities were completed and tested. The cavity cells were fabricated from 4 mm thick, high purity niobium (RRR=208) with a yield strength of 50-59 MPa and elongation of 44-48%. A reentrant half-cell can be seen in Figure 2. The beam tubes were fabricated from 2 mm thick niobium (RRR=197) with a yield strength of 56-60 MPa and elongation of 45-58%. All niobium was supplied by Tokyo Denkai. The beam tubes were chosen

to be 2 mm thick for cost savings after analysis predicted a maximum Stress Von Mises of 27 MPa in a very localized region near the reentrant iris. For the analysis, 1 bar pressure differential was used (vacuum inside the cavity, ambient pressure outside) with "fixed-free" boundary conditions and a beam tube thickness of 1.62 mm to account for thinning from machining and etching. These results indicate there may be plastic deformation in a localized region after the cavity is post-purified, which would reduce the yield strength by approximately a factor of two. Our predictions show that while a single-cell half-reentrant cavity may plastically deform in a localized region near the iris after post-purification during a "fixed-free" test, the cavity will be safe from collapse.

The beam tubes were chosen to be 12.675 cm long, and with this length, simulations indicate a 0.025% reduction of Q_o at 1.5 K due to losses in the stainless steel endcaps. The flanges are NbTi using 11.7 cm knife edge seals with copper gaskets.

Deep Drawing

Deep drawing was done with the regular two-step process with each half-cell pressed with 75 tons followed by coining dies pressed with 17 tons. We did not notice any tearing of the initial copper test blanks, even with small inner diameter holes. The outer edge of the niobium was constrained with the proper torque on the hold-down bolts. No intermediate anneals were performed. Following the advice offered by Cornell taken from their experience fabricating reentrant cavities, vent holes were drilled in the reentrant region for both the female and male dies to allow lubrication to escape during stamping. The half-cells were trimmed and interlocking equator and iris joints were machined.

Figure 2: Reentrant half-cell with checking fixture.

Electron-beam Welding

All electron-beam (e-beam) welds were done at Sciaky Corporation in Chicago with a 50 kV welder. The beam tubes were rolled, stamped, and then e-beam welded length wise with a full penetration weld of the butt joint. The tubes were then e-beam welded to the NbTi flanges using a very focused beam to minimize alloying of titanium into the niobium beam tubes. The iris was tack welded to the beam tubes and then welded from the inside at an angle of 30° using a 25.4 cm gun-to-work distance, 38 mA, and 45.7 cm/minute. This was followed by a weld from the outside, perpendicular to the beam axis, using a 20.3 cm gun-to-work distance, 38 mA, and 45.7 cm/minute. The full penetration equator weld was performed from the outside through 0.13 mm thick niobium. The equator weld used an oscillation of 1 kHz, maximum spot diameter of 0.13 mm, and gun-to-work distance of 20.3 cm. Tack welds were completed with 18 mA at 45.7 cm/minute, followed by a seal pass with 38 mA at 45.7 cm/minute. The main e-beam weld was then done for cavity 1 with 48 mA, 30.5 cm/minute. The weld did not fully penetrate, so the cavity was rewelded with 55 mA, 30.5 cm/minute. Cavity 2 was e-beam welded one time with 51 mA, 30.5 cm/minute. While the weld for cavity 2 was sufficient, we plan to use 53 mA for the main equator weld for future cavities.

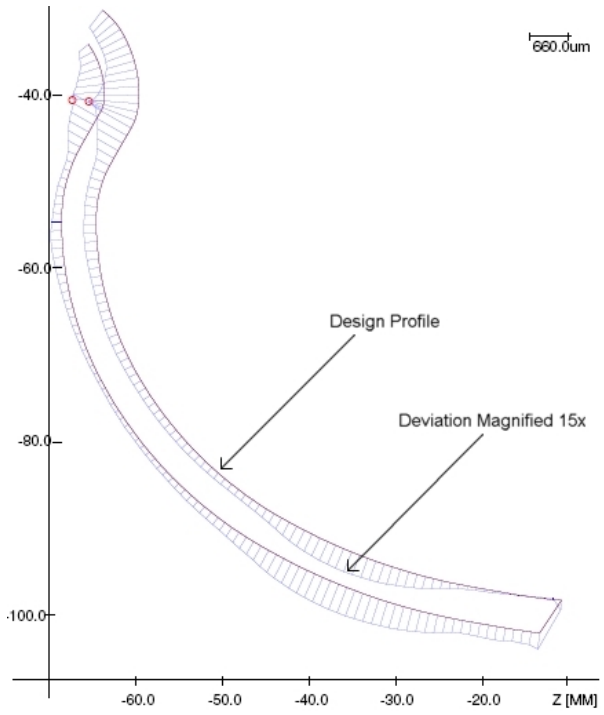

Figure 3: Coordinate measurement of reentrant half-cell after iris weld.

Coordinate Measurement

The half-reentrant cavity profile was measured at two different times during the fabrication process by a Zeiss

Prismo 10 Vast HTG 2400 at Advanced Consulting and Engineering. The first coordinate measurement was done after the reentrant and non-reentrant half-cells were stamped, before any machining. A second coordinate measurement was performed after the iris weld, and the results can be seen in Figure 3. The equatorial plane of the machined equator step is used as the reference for the second coordinate measurement. Based off of this reference, the maximum deviation of the fabricated shape from the design shape is 0.84 mm and occurs near the iris at the location of the red circles. However, this equatorial reference plane is not absolute, as there will be machining errors in the machined weld prep. One can shift the reference to better align the coordinate measurement profile with the design shape. If this is done, the maximum deviation of the fabricated shape from the design shape, before the equator weld, is reduced to 0.35 mm and is within our goal of 0.51 mm. The effect of the iris weld on the cavity shape should be negligible, since it is not a full penetration weld. Indeed, the two coordinate measurements showed a small change in the cavity shape near the iris of less than 0.07 mm.

There was thinning from 4 mm to 3.71 mm as well as a sharp transition in the cavity profile near the iris where the coining die was pressed. This could perhaps be avoided by increasing the radius of the coining die and thus providing a more continuous transition. One can also see the expected material thickening near the equator. A 0.51 mm allowance for weld shrinkage was designed into the equator prep, however actual weld shrinkage ranged from 0.61 mm to 1.02 mm.

CAVITY PREPARATION

Etching at MSU was done with a buffered chemical polish (BCP) solution of HF, HNO_3, and H_3PO_4 in a volumetric ratio of 1:1:2. For an interior etch, teflon flanges are bolted to either end of a single-cell cavity, and the cavity is then attached in a vertical position to the BCP system within the chemistry room. Given a known etch rate at a given temperature (typically 1-2 um/min at 18 C), a BCP solution is pumped through the inside of the cavity for a given period of time until the desired thickness of niobium is removed. The acid is then drained from the cavity and the cavity is rinsed with ultra-pure water for 10 minutes to remove any iota of acid. The cavity is then filled with ultra-pure water and let sit for 60 minutes.

The exteriors of both half-reentrant cavities were etched in an attempt to improve the thermal conductivity by removing any contaminants from the outside surface. Exterior etching was done by taping the beam tubes and ends of the cavity with teflon tape and then laying the cavity horizontally in a bath of BCP (see Figure 4). The bath of BCP was immersed in an ice bath and placed inside the glove box in the chemistry room. Since the cavity was only partially immersed, it was rapidly manually rotated in an effort to keep the entire surface wet for the majority of the time. Our goal was to remove 50 um from the exterior, and since

Figure 4: Half-reentrant cavity during exterior etch in chemistry room.

we estimated a removal rate of 2 um/min, the cavities were etched for 26 minutes plus an additional amount of time while the glove box panel was removed. The cavities were rinsed in a water bucket and then running water. All exterior discoloration went away with the exterior etches.

Figure 5: A half-reentrant cavity is shown during an interior etch on the left and during a high-pressure rinse (HPR) on the right.

A half-reentrant cavity can be seen during an interior etch and high-pressure rinse in Figure 5. A summary of the surface preparation of the two single-cell half-reentrant cavities at MSU can be seen in Table 3. After the tests at MSU were complete, cavity 5/6 was sent to TJNAF. This cavity underwent ultrasonic degreasing in a water/detergent solution for approximately 30 minutes, and then was post-purified at 1250 C for 3 hours in a titanium box. To prevent potential deformation of the half-reentrant cavity, the cavity was initially constrained. However, the assembly of the cavity with the stiffeners was quite difficult, and a contamination-free assembly could not be accomplished which ultimately led to poor test results (E_{acc}^{max}=13.8 MV/m in the first test and 18.9 MV/m in the second). The decision was then made to remove the con-

straints and retest the cavity a third time. It is these test results that are shown in Table 3 and Figure 6.

Table 3: Summary of cavity surface preparation for single-cell half-reentrant cavities before each test and maximum fields attained. Cavity 5/6 is fabricated from half-cells 5 and 6. Cavity 2/3 is fabricated from half-cells 2 and 3. The intrinsic quality factor (Q_o) listed is the value when the cavity quenched.

Cavity 5/6	Cavity 2/3
Surface Preparation: BCP interior 180 um HPR 90 minutes	Surface Preparation: BCP exterior 50 um BCP interior 180 um HPR 64 minutes
1.5 K Test Results August 2006: E_{pk}=35.6 MV/m E_{acc}=15.7 MV/m B_{pk}=55.31 mT Q_o=1.4E10 X-ray level = 200 mR/hr	1.5 K Test Results January 2007: E_{pk}=38.2 MV/m E_{acc}=16.8 MV/m B_{pk}=59.2 mT Q_o=4.4E9 X-ray level = 0 mR/hr
Surface Preparation: BCP exterior 50 um BCP interior 135 um HPR 65 minutes	
1.5 K Test Results February 2007 E_{pk}=55.8 MV/m E_{acc}=24.6 MV/m B_{pk}=86.6 mT Q_o=2.0E9 X-ray level = 2 mR/hr	
Cavity Sent to TJNAF Surface Preparation: Post-purification BCP interior 60 um HPR	
2 K Test Results July 2007 E_{pk}= 80.1 MV/m E_{acc}=35.3 MV/m B_{pk}= 124.3 mT Q_o= 1.0 E10 No Field Emission	

TEST RESULTS

A total of three tests were completed for two single-cell half-reentrant cavities at MSU. Cavity 5/6 consists of half-cells 5 and 6, and was tested in August of 2006 and again in February of 2007 at MSU. Cavity 2/3 consists of half-cells 2 and 3, and was tested in January of 2007 at MSU. In July 2007, Cavity 5/6 was post-purified and tested at TJNAF. A summary of the tests with the surface preparation techniques and highest achieved fields can be seen in Table 3 and the Q-Curve for various tests at 2 K is in Figure 6.

The first tests of cavity 5/6 and 2/3 reached an accelerating gradient of roughly 15 MV/m - 16 MV/m. X-rays were observed during the initial testing of cavity 5/6 while cavity 2/3 was field-emission free. Cavity 5/6 received an additional interior etch along with an exterior etch and when retested, reached an accelerating gradient of 24.6 MV/m. All tests were limited in field by quench. The low-field Q_o was measured as a function of temperature, and the residual surface resistance was found to be between 7 nΩ and 13 nΩ.

These test results are in good agreement with other single-cell niobium cavities having undergone similar surface preparation at MSU. However, there may be two advantages seen from initial testing of the half-reentrant cavities: field-emission free cavities and the onset of high-field Q-slope at relatively high fields. All tests showed either no field-emission or relatively little field emission, which may be due to the 8° wall angle on the non-reentrant half of the cavity allowing for proper drainage of fluids.

In traditional elliptical cavities having undergone BCP and then post-purification, high-field Q-slope typically improves after low-temperature baking. In our case, the post-purified but unbaked half-reentrant cavity did not exhibit high-field Q-slope until B_{pk} = 120 mT, and the Q-slope seen is somewhat mild. The Q-slope beginning at 120 mT is most likely the onset of high-field Q-slope. The first tests of single-cell reentrant cavities [9] were not tested under the same circumstances (i.e. all cavities were post-purified and baked before testing), and therefore cannot provide a true comparison. The final test of the half-reentrant cavity seems to show a lack of high-field Q-slope below B_{pk} = 120 mT, which is somewhat remarkable for an unbaked cavity.

Frequency Shifts

Fluctuations in bath pressure, variations in cavity temperature, Lorentz force detuning, and cavity tuning will all cause small deformations in the cavity shape and therefore cause the frequency of a cavity to shift. These frequency shifts need to be understood before the final multi-cell fabrication begins so that the design frequency can be reached at the operating temperature and pressure. Structural analysis of the half-reentrant cavity was done by E. Zaplatin and can be found in [10]. Changes in bath pressure and Lorentz force detuning are discussed here.

Changes in Bath Pressure The frequency drop was measured in all three half-reentrant tests at MSU and can be seen in Figure 7.

The frequency shift due to 1 bar external pressure as a function of wall thickness was predicted by E. Zaplatin [10] and is shown in Figure 8. According to Figure 8, the frequency shift due to a pressure differential across the cavity wall is -125 kH/bar at a wall thickness of 3.7 mm (the

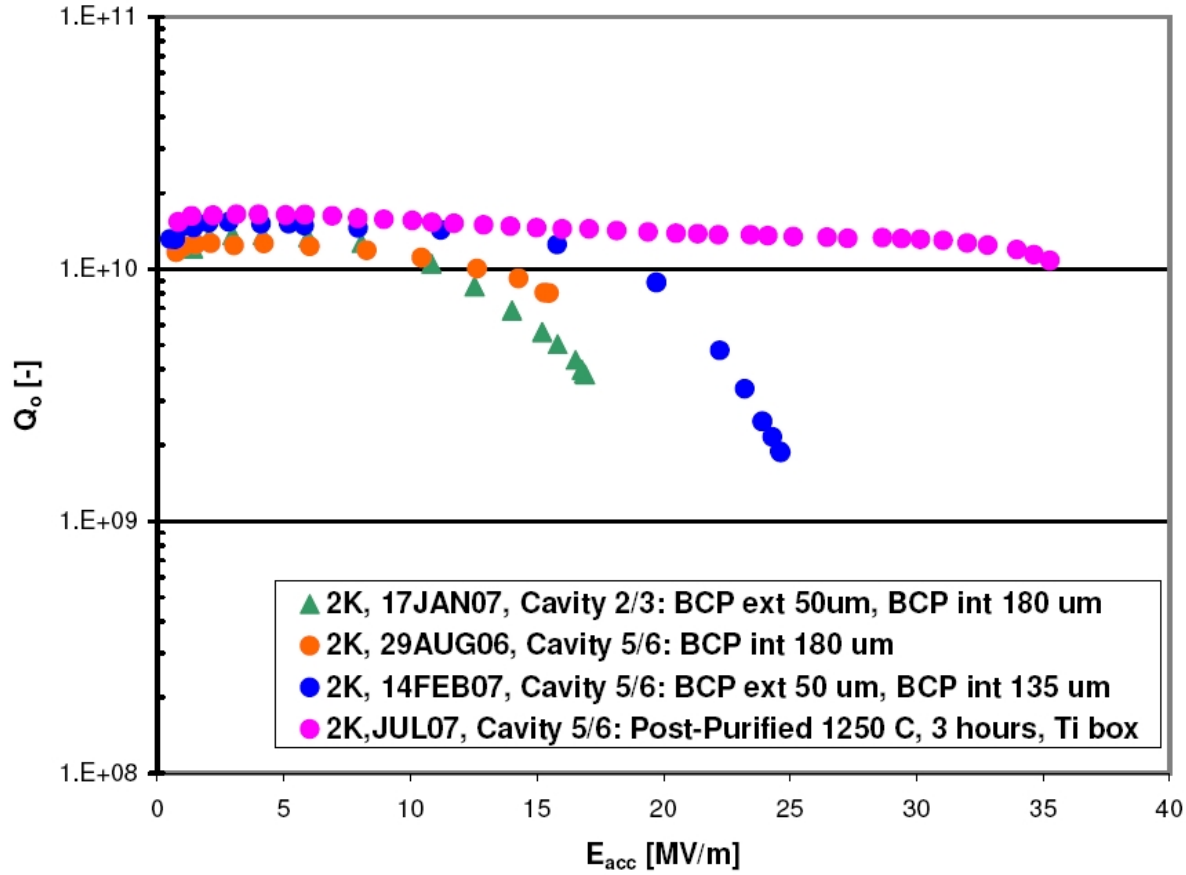

Figure 6: Test results of two half-reentrant single-cell prototypes at 2 K. All tests were limited in field by quench.

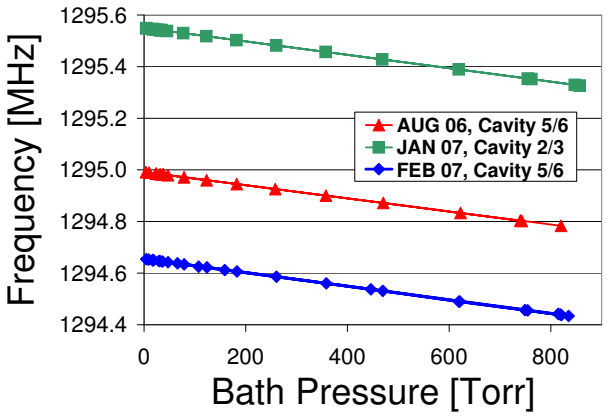

Figure 7: Plot of frequency versus pressure for the three tests at MSU.

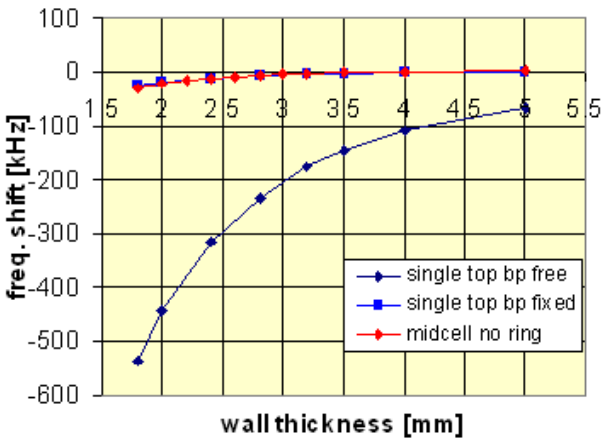

Figure 8: Plot of frequency versus wall thickness for 1 bar external pressure [10]. We see the predicted df/dP is much smaller when both beam tubes are fixed compared to the case of one free beam tube. Therefore df/dP for a multi-cell half-reentrant cavity in a cryomodule might be significantly smaller than what is measured for a single-cell with one beam tube free.

final wall thickness near the iris as determined by the coordinate measurement). This is equivalent to -166.6 Hz/torr, which is in reasonable agreement with the measured values of -254.5 to -264.5 Hz/torr, taking into consideration the measured thickness of the cavity wall varies as a function of position.

Moreover, the frequency shift due to external pressure is a function of the wall thickness and can be measured

for a cavity as it is progressively etched and made thinner. Table 4 shows the trend that as the cavity wall becomes thinner, the same differential pressure will have a larger effect on the frequency shift. We can compare these test results to the predictions by assuming a linear change in the frequency shift for a wall thickness between 3.5 mm and 4 mm in Figure 8. This gives a frequency shift of -53.3 Hz/Δmm torr, meaning that for every mm of material that is removed, the frequency shift will be lowered by 53.3 Hz for a pressure differential of 1 torr. Table 4 shows the second test of Cavity 5/6 had 185 um more material removed than the first test of Cavity 5/6, and a change in df/dP of 10 Hz/torr, corresponding to a frequency shift of Hz/Δmm torr, which is in good agreement of the predicted value of -53.3 Hz/Δmm torr.

Table 4: Measured frequency shift for a given pressure differential as measured for the three half-reentrant cavity tests at MSU.

	Material removed after equator weld	df/dP [Hz/torr]
Cavity 5/6, Aug 2006	180 um	-254.54
Cavity 2/3, Jan 2007	230 um	-260.52
Cavity 5/6, Feb 2007	365 um	-264.53

Lorentz Force Detuning The measured Lorentz force detuning coefficient (K_L) for the half-reentrant single-cell was found to be between $-6\ \frac{Hz}{\frac{MV}{m}^2}$ and $-7\ \frac{Hz}{\frac{MV}{m}^2}$. This is in agreement with other single-cell elliptical cavities. The predicted K_L for the mid-cell geometry with no stiffening rings was found to be $-0.5\ \frac{Hz}{\frac{MV}{m}^2}$. Furthermore, simulations show that the half-reentrant, TeSLA, low-loss, and reentrant mid-cell shapes all have similar Lorentz force detuning coefficients [11].

CONCLUSION

Two single-cell half-reentrant niobium cavities have been fabricated and tested at MSU, with one cavity post-purified and tested at TJNAF. Coordinate measurements show the cavity shape to be within 0.41 mm of the design profile before the equator weld. Multipacting simulations do not predict hard barriers. First test results show a half-reentrant cavity having undergone only BCP and post-purification can reach E_{acc}=35 MV/m with the onset of high-field Q-slope occurring no earlier than B_{peak} = 120 mT. Mechanical analysis has been done for a multi-cell half-reentrant cavity and the Lorentz force detuning predictions are comparable to reentrant and low-loss shapes. We anticipate that the half-reentrant cavity will be able to reach a higher gradient with electropolishing and further testing.

ACKNOWLEDGMENTS

We thank our colleagues, particularly J. Sekutowicz for useful discussions about cavity design shapes, R. L. Geng and T. Saeki for useful discussions and comments about the fabrication process, and H. Padamsee for suggestions made during testing.

REFERENCES

[1] J. Sekutowicz et al., "Design of a Low Loss SRF Cavity for the ILC", Proceedings of the 2005 Particle Accelerator Conference, Knoxville, Tennessee.

[2] V. Shemelin et al., "An Optimized Shape Cavity for TESLA: Concept and Fabrication", Proceedings of the 2003 Particle Accelerator Conference, Portland, Oregon, pp. 1314-1316.

[3] M. Meidlinger et al., "Design of Half-Reentrant SRF Cavities", Physica C, Volume 441, Issues 1-2, July 2006, pp. 155-158. Also published in the Proceedings of the Twelfth International Workshop on RF Superconductivity", Ithaca, New York, 2005.

[4] R.L. Geng, "Review of New Shapes for Higher Gradients", Proceedings of the 12th International Workshop on RF Superconductivity, Ithaca, New York, July 10-15, 2005.

[5] D.G. Myakishev and V. P. Yakovlev, "The New Possibilities of SuperLANS Code for Evaluation of Axisymmetric Cavities", Proceedings of the 1995 Particle Accelerator Conference, IEEE Publishing, Piscataway, New Jersey, pp. 2348-2350, 1996.

[6] D.G. Myakishev and V. P. Yakovlev, "An Interactive Code SUPERLANS for Evaluation of RF-Cavities and Acceleration Structures", Conference Record of the 1991 IEEE Particle Accelerator Conference, IEEE Publishing, Piscataway, New Jersey, pp. 3002-3004, 1991.

[7] R. Ferraro, R. Kahn, W. Hartung, T. G. Flynn, S. Belomestnykh, "Guide to Multipacting/Field Emission Simulation Software", Sixth Edition, Report SRF/D-961126/10, Laboratory of Nuclear Studies, Cornell University, Ithaca, NY, 1996.

[8] W. Hartung, F. Krawczyk, H. Padamsee, "Studies of Multipacting in Axisymmetric Cavities for Medium-Velocity Beams", Proceedings of the Tenth Workshop on RF Superconductivity, Tsukuba, 2001, KEK Proceedings 2003-2 A, KEK, Tsukuba, Japan, June 2003, p. 627-631.

[9] R. L. Geng, H. Padamsee, A. Seaman, J. Sears, V. Shemelin, "Testing the First 1300 MHz Reentrant Cavity", Proceedings of the Workshop of Pushing the Limits of RF Superconductivity, Argonne National Laboratory, September 22-24, 2004. Also published as Report SRF041014-04, Laboratory of Elementary Particle Phsyics, Cornell University, Ithaca, NY, 2004.

[10] E. Zaplatin, T. L. Grimm, W. Hartung, M. Johnson, M. Meidlinger, J. Popielarski, "Structural Analysis for a Half-Reentrant Superconducting Cavity", Proceedings of Tenth European Particle Accelerating Conference, pp. 424-426, 2006.

[11] E. Zaplatin et al., "Lorentz Force Detuning Analysis for Low-Loss, Reentrant, and Half-Reentrant Superconducting RF Cavities", Proceedings of LINAC 2006, Knoxville, TN, pp. 734 - 736.